Published in final edited form as:
J Am Chem Soc. 2010 February 17; 132(6): 2016–2023. doi:10.1021/ja909303g.

Paramagnetic, silicon quantum dots for magnetic resonance and two photon imaging of macrophages

Chuqiao Tu[†], **Xuchu Ma**[†,‡], **Periklis Pantazis**[§], **Susan M. Kauzlarich**[‡,*], and **Angelique Y. Louie**[†,*]

[†]Department of Biomedical Engineering, University of California, Davis, CA 95616, USA

[‡]Department of Chemistry, University of California, Davis, CA 95616, USA

[§]Biological Imaging Center, Beckman Institute, California Institute of Technology, Pasadena, CA 91125, USA

Abstract

Quantum dots (QDs) are an attractive platform for building multimodality imaging probes, but the toxicity for typical cadmium QDs limits enthusiasm for their clinical use. Nontoxic, silicon QDs are more promising but tend to require short wavelength excitations which are subject to tissue scattering and autofluorescence artifacts. Herein, we report the synthesis of paramagnetic, manganese-doped, silicon QDs ((Si_{Mn} QDs) and demonstrate that they are detectable by both MRI and near infrared excited, two-photon imaging. The Si_{Mn} QDs are coated with dextran sulfate to target them to scavenger receptors on macrophages, a biomarker of vulnerable plaques. TEM images show that isolated QDs have an average core diameter of 4.3 ± 1.0 nm and the hydrodynamic diameters of coated nanoparticles range from 8.3 to 43 nm measured by Dynamic Light Scattering (*DLS*). The Si_{Mn} QDs have an r_1 relaxivity of 25.50 ± 1.44 $mM^{-1}s^{-1}$ and an r_2 relaxivity of 89.01 ± 3.26 $mM^{-1}s^{-1}$ (37 °C, 1.4 T). They emit strong fluorescence at 441 nm with a quantum yield of 8.1% in water. Cell studies show that the probes specifically accumulate in macrophages by a receptor-mediated process, are nontoxic to mammalian cells, and produce distinct contrast in both T_1-weighted magnetic resonance and single- or two-photon excitation fluorescence images. These QDs have promising diagnostic potential as high macrophage density is associated with atherosclerotic plaques vulnerable to rupture.

Introduction

Current interest in the development of non-invasive molecular imaging has shifted towards multimodality imaging, as no single imaging modality possesses all of the ideal traits of being quantitative, longitudinal (to allow imaging over time), and providing both high resolution and sensitivity.1 The combination of non-ionizing magnetic resonance imaging (MRI) and optical techniques has attracted attention because of their highly complementary capabilities for anatomical resolution and detection sensitivity.2 The hybrid modality has shown potential for significantly increased diagnostic accuracy compared to standalone imaging and is leading to increasing interest in multifunctional materials that can be detected by both modalities. Nanomaterials are ideal for this purpose as they provide a particularly useful platform to integrate multiple functionalities into a single entity. One logical approach that has emerged is to build multimodal probes for MR/optical imaging based on quantum dots (QDs).3,4

aylouie@ucdavis.edu. smkauzlarich@ucdavis.edu.

Supporting Information Available: FT-IR spectrum and emission spectra of DS Si_{Mn} QDs, etc. This material is available free of charge via the internet at http://pubs.acs.org.

QDs have been widely used for biomedical imaging over the last decade.[5] Their use as laboratory research tools has grown tremendously but enthusiasm for their clinical application has been limited due to concerns about possible toxicity.[6] Silicon QDs are expected to be an ideal candidate in many biological applications because of their proven biocompatibility.[7] However, to date most Si QDs reported are of single functionality used solely for fluorescence imaging.[8–11] An effective method for providing QDs with magnetic properties is magnetic impurity doping and we have previously demonstrated that CdSe QD containing paramagnetic ions can be detected by both MR and fluorescence imaging.[12]

Recently we doped manganese (Mn) into Si QDs *via* a low-temperature solution route. This work indicated that the Mn-doped QDs (Si_{Mn} QDs) possess both favorable optical and magnetic properties and thus show potential for use in combined MR/optical imaging.[13] However, the Si_{Mn} QDs prepared were surface-passivated with octyl groups and were not water-soluble. For Si_{Mn} QDs to be used in biomedical imaging they must be water soluble to prevent aggregation and precipitation in a biological environment, and ideally should be tissue- or biomarker-targeted so that they will accumulate in specific tissues or organs and allow for an improved diagnosis of these body regions. In this work, we develop a new synthetic route to generate water soluble, paramagnetic Si_{Mn} QDs. These dual-functional QDs are coated to target to atherosclerotic plaques, with the ultimate goal of diagnosing plaque stability.

Increasing evidence indicates that it is plaque rupture rather than severity of occlusion that leads to acute infarction or sudden cardiac death. Considerable interest exists in detection of these vulnerable plaques in early stages; however, sensitive detection and differentiation of vulnerable versus stable atherosclerotic plaques in vessels with mild-severity stenoses remains limited.14 There is evidence that composition and presence of specific markers can indicate if a plaque is at risk for rupture.14 For example, a higher density of macrophages in plaques has been correlated with instability and localization to the plaque shoulders indicates greater risk of rupture.[15] To image macrophage density we target our probes to the macrophage scavenger receptor class A (SR-A), a cell surface receptor primarily expressed by mature macrophages.[16] Targeting is achieved by coating the Si_{Mn} QDs with dextran sulfate (DS), a ligand for macrophage SR-A.[17] The uptake of DS coated, Mn-doped Si QDs (DS Si_{Mn} QDs) by cultured macrophages was evaluated and cytotoxicity was tested. Receptor-mediated uptake is confirmed by control experiments with nontargeted QDs and competitive inhibition experiments. Significant contrast enhancement can be observed by both MR and near infrared (NIR) two-photon imaging, indicating the promise of DS Si_{Mn} QDs for biological applications.

Experimental Section

General

Reagents were obtained from commercial suppliers and used directly, unless otherwise noted. Dry solvents, where indicated, were obtained from either Aldrich or Fisher Scientific as anhydrous Sure-Seal bottles. Water was purified using a Millipore Milli-Q Synthesis purifier (18.0 MΩ cm, Barnstead). pH value was measured with a Beckman Φ240 pH/Temp meter. The absorption spectra were taken with a Cary 100-Bio UV-vis spectrophotometer. Emission spectra were recorded with a FluoroMax-P (JOBIN YVON Inc.). Powder X-ray diffraction (XRD) data were collected on Mn-doped Na_4Si_4 and the solid product using an air sensitive holder on a Bruker D8 Advance X-ray diffractometer operating at 40 kV and 40 mA with Cu*K*α radiation (λ = 1.54178 Å). TEM was performed on a Philips CM-12, operating at 80 kV. DLS was used to determine the overall particle size in solution with a Nanotrac 150 particle size analyzer (Microtrac, Inc., Montgomeryville, PA). Elemental analysis was performed by Columbia Analytical Services of Tucson, Arizona. FT-IR spectra of QDs were collected on a Shimadzu IR Prestige 21 spectrophotometer.

Preparation and characterization of water-soluble Mn-doped Si (Si_{Mn}) QDs

Mn-doped Si QDs were prepared from the precursor of 1% Mn-doped sodium silicide, which was synthesized according to a modified procedure published for sodium germanide.[18,19] All chemicals were handled either in a N_2-filled glovebox or on a Schlenk line using standard anaerobic and anhydrous techniques. Unless otherwise stated, all powders are oxygen-sensitive and precautions must be taken to avoid exposure to oxygen. A high-energy Spex 8000M mill with a tungsten carbide milling vial and two tungsten carbide balls (diameter of ~ 1 cm) was used to ball-mill mixtures of NaH, Si and Mn powders with an appropriate molar ratio. The milling was performed for about 30 minutes, which resulted in a uniformly ground powder. Briefly, a pre-milled mixture of NaH, Si and Mn (molar ratio of 1.9:0.99:0.01) was placed into an alumina crucible with a lid, and placed into a quartz tube with stopcocks on both ends. The tube was removed from the glovebox and placed in a tube furnace and connected to purified nitrogen gas with a mineral oil bubbler outlet. The quartz tube was heated at 420 °C for 2 days followed by heating at 500 °C for 1 additional day under flowing nitrogen. The X-ray powder diffraction of the final black powder product was consistent with the sodium silicide crystal structure.[20]

Glassware was dried overnight at 120 °C and transferred hot into an N_2-filled glovebox. *N*,*N*-dimethylformamide (DMF) was degassed and NH_4Br was dried at 100 °C under vacuum and stored in a glovebox. DMF (100 mL) was added *via* cannula to Mn-doped sodium silicide (0.204 g, 4 mmol) and NH_4Br (0.784 g, 8 mmol) in a three-neck bottle and heated to reflux for 2 hours under nitrogen. After the reaction mixture was cooled to room temperature, 2 mL of allylamine was added and the reaction mixture was heated to reflux for 2 hours while stirring. This mixture was allowed to cool to room temperature and a black solid along with a yellow solution was obtained. The yellow solution was transferred and dried utilizing a rotavap and an orange solid was obtained. The resulting orange product was dissolved in 15 mL of nanopure water and centrifuged in a dialysis bag to remove any impurity. The precursor Mn-doped sodium silicide and the aqueous solution containing propylamine capped Mn-doped Si QDs was characterized by XRD, TEM, and FT-IR.

Coating of dextran sulfate or dextran on the Mn-doped Si QDs

DMSO/pyridine (75 mL, l/l (v/v)) was added to a flask containing dextran sulfate (1.047 g, 1.9 mmol of hydroxyl groups, MW/MN = 6,500–10,000 Da, 17% S) and 4-nitrophenyl chloroformate (0.875 g, 4.341 mmol) at 0 °C and argon atmosphere. A 10 mol % (*vs* chloroformate, 0.054 g, 0.434 mmol) solution of DMAP was added as a catalyst. The reaction mixture was stirred under argon for 4 hrs at 0 °C. The reaction product was isolated by precipitation in 300 mL of ether/ethanol (1/1, v/v). The precipitate was isolated by filtration and washed with ethanol/ether (l/l, v/v) and then with ether. The 4-nitrophenyl-activated dextran sulfate was dissolved in 150 mL of DMSO/pyridine (2/1, v/v) and then Mn-doped Si QDs prepared above were added to the flask. The mixture was stirred under argon for 48 h. After the solution was concentrated, the residue was dissolved in water and was dialyzed against deionized water in a dialysis bag with MW cut-off of 12,000–14,000 Da for 72 h (8–10 changes of water) to yield 0.297 grams of pale yellow solid. IR: 3580 (N-H stretch), 3048 (tertiary C-H stretch), 2924 & 2847 (secondary C-H stretch), 1713 (C=O), 1582 (secondary amide N-H bending), 1258 (asymmetric S=O stretch) and 1018 cm^{-1} (symmetric S=O stretch). Elemental analysis: C 18.6%, H 3.75%, N 1.51%, S 9.62%. The amount of manganese in DS Si_{Mn} QDs was measured on an atomic absorption (AA) spectrophotometer Varian AA 220FS using an air/acetylene flame, which is 1.5 mg/L of manganese when 97.17 mg of DS Si_{Mn} QDs was dissolved in 4 mL of deionized water containing 3% of hydrochloric acid. The preparation of dextran-coated (D) Si_{Mn} QDs is the same as described above except for using 1.5 equivalent of 4-nitrophenyl chloroformate.

Confocal and 2-Photon Microscopy

Aqueous solutions and cells containing DS Si_{Mn} QDs or D Si_{Mn} QDs were imaged with a Zeiss LSM 5 Pascal confocal microscope for single-photon microscopy and a Zeiss LSM 510NLO microscope for two-photon microscopy, respectively. In single-photon microscope an excitation wavelength of 405 nm (25% power) was used with a 405/514 nm HFT beam splitter, and a 420 nm low pass filter. In two-photon microscope signal profiles of DS Si_{Mn} QDs covering the spectral range from 380 to 720 nm were recorded using the META detector by tuning the wavelength from 780 to 900 nm.

Relaxivity

Longitudinal (T_1) and transverse (T_2) relaxation times were measured at 60 MHz (1.4 T) and 37 °C on a Bruker Minispec mq60 (Bruker, Billerica, MA). Two stock solutions of DS Si_{Mn} QDs or D Si_{Mn} QDs were prepared by dissolving appropriate amount of QDs in pH 7.0 deionized water. The concentration of Mn was determined by atomic absorption (AA). All solutions were prepared by weight. Mn concentrations were calculated based on the concentration of the stock solution and appropriate dilution factors. The stock solutions were diluted respectively to give two series of aqueous solutions with decreasing Mn(II) concentration (0.4 mL each with Mn concentrations between 0.008 and 0.12 mM). T_1 values were measured using an inversion recovery sequence with 10–15 data points and T_2 values were measured using a Carr–Purcell–Meiboom–Gill (CPMG) sequence with $\tau = 1$ ms, and 200 data points. Each solution was incubated at 37 °C for 10 min before measurement. The longitudinal (r_1) and transverse (r_2) relaxivity were determined as the slope of the line for plots of $1/T_1$ or $1/T_2$, respectively, against increasing manganese concentration with a correlation coefficient greater than 0.99.

Magnetic Resonance Imaging (MRI)

MRI was performed on an Avance 400 system (400 MHz (9.4 T), 21 °C, Bruker, Billerica, MA). The magnet was equipped with the standard gradient set and 25 mm internal diameter (ID) volume coil. Aqueous solutions of DS Si_{Mn} QDs or D Si_{Mn} QDs were prepared as described in the relaxivity measurement section. Parameters for the images were TR = 1000 ms, TE = 15 ms for T_1 weighted (T_1W) images, and TR = 6000 ms, TE = 42 ms for T_2 weighted (T_2W) images. For all images a spin echo sequence was used with a field view (FOV) of 2.8 cm^2, slice thickness 1.0 mm, and a 128 × 128 matrix. The cell lysates were imaged by the same procedure as solutions.

Dextran Sulfate or dextran coated Mn-doped Si QDs Uptake by P388D1 Cells (Mouse Macrophages)

P388D1 cells were plated at 5×10^5 cells/mL (2 mL per dish, 70 mm diameter) and maintained in media (RPMI-1640 with L-Glutamine and 10% LPDS) at 37 °C in a 5% CO_2 atmosphere overnight which allowed cells to adhere to the dishes. Solutions of DS Si_{Mn} QDs or D Si_{Mn} QDs ($[Mn^{2+}] = 2.0 \times 10^{-5}$ M) in the same media were prepared and incubated in 37 °C water bath for 20 min before use. After removal of media, nanoparticle containing solutions were introduced to the cells and incubated at 37 °C in 5% CO_2 atmosphere for 1 h. After removal of the media containing probes, cells were washed three times with 1X PBS and placed in PBS for confocal imaging or for the MR sample, 1 mL of nanopure water was added, and the freeze-thaw method was repeated three times to lyse cells. Cell lysate was put into a 1.5 mL conical tube, concentrated by freeze-drying (speed vacuum) to 0.25 mL, and used for MRI.

For cell fixation, a glass slide was dipped in collagen I acetic acid solution in a 70 mm diameter dish for one hour. The collagen solution was removed and the glass slide was washed three times with 1X PBS. DS Si_{Mn} QDs containing solutions were added to the dish and the dish

was put in the oven (37 °C, 5% CO_2 atmosphere) for 1 h. After removal of the media containing DS Si_{Mn} QDs, cells were washed three times with 1X PBS, then fixed with 10% formaldehyde PBS solution for 2-photon imaging.

Specificity of Uptake

To verify that uptake was specific, P388D1 cells in RPMI-1640 were plated at 5×10^5 cells/mL and incubated with either dextran sulfate- or control of dextran-labeled with Mn-doped Si QDs. Dextran is not recognized by the scavenger receptor. The dextran sulfate-coated and dextran-coated QDs used here were prepared by the same method and with same batches of Mn-doped Si QDs. Similar manganese load was confirmed by AA. Cells were incubated at 37 °C in a 5% CO_2 atmosphere for 1 h and then prepared for imaging as described before. To verify that cellular uptake was receptor-specific, competition experiments were conducted and characterized by confocal microscopy and MRI. Cells were incubated with DS Si_{Mn} QDs ($[Mn^{2+}] = 1.64 \times 10^{-5}$ M) in the presence of dextran sulfate as competitor in 0, 0.1, 1, and 10-fold excess concentrations. The MW of the dextran sulfate coated Mn-doped Si QDs was estimated based on the results of elemental analysis (C 18.6%, H 3.75%, N 1.51%, S 9.62%). Cells were incubated at 37 °C in a 5% CO_2 atmosphere for 1 h and then prepared for imaging as described before.

Toxicity

Cytotoxicity of DS Si_{Mn} QDs was evaluated with two mammalian cell lines by through the use of C_{12} - Resazurin viability assays (Invitrogen). P388D1 cells in RPMI-1640 or mouse embryonic fibroblast NIH 3T3 cells in Dulbecco's Modified Eagle's Media (DMEM) were plated in 96-well dishes at a concentration of 1.1×10^4 cells per well. This places the cells at a density for linear growth rate which is optimal for the assay.[21] After overnight incubation (37°C, 5% CO_2), the existing RPMI-1640 or DMEM was replaced with fresh media containing varying amounts of probes. For NIH 3T3 cells, 62.71 mg of DS Si_{Mn} QDs was dissolved in 0.6 mL of medium. The resultant solution and medium were added into wells 1 to 6 to form a series of QDs solutions. Therefore, the mass of DS Si_{Mn} QDs in wells 1 to 6 are 0, 0.65, 1.31, 2.61, 5.22, and 10.45 mg. For P388D1 cells, 61.18 mg of DS Si_{Mn} QDs was dissolved in 0.6 mL of medium. Therefore, the mass of DS Si_{Mn} QDs in wells 1 to 6 are 0, 0.64, 1.27, 2.55, 5.10, and 10.20 mg. Cells were incubated with probes for 24 hours. The media were removed and cells were washed with 1X PBS three times, then media containing C_{12} - Resazurin (5 μM) was added. After incubation for 15 minutes for reduction of the compound, fluorescence was measured using a Safire^2 monochromator microplate reader (Tecan Austria G.M.B.H., Austria) with excitation of 563 nm and an emission of 587 nm. Samples were performed in triplicate to provide statistical significance.

Results and Discussion

1. Synthesis and characterization of Si_{Mn} QDs

The 1% Mn-doped sodium silicide precursor was synthesized according to a modified procedure with a pre-milled mixture of NaH, Si and Mn (molar ratio of 1.9:0.99:0.01) (Figure 1a).[18] The X-ray diffraction (XRD) pattern of the as-prepared Mn-doped sodium silicide is consistent with the calculated Na_4Si_4 powder pattern (Figure 1b). There are no unindexed peaks that could be attributed to Na, NaH, Si, Mn or any other impurities. Lattice parameters determined by Rietveld refinement of the XRD pattern are a = 12.1613(31) Å, b = 6.5494(33) Å, c = 11.1364(31) Å, and β = 118.9509(92) °, consistent with the published lattice parameters of Na_4Si_4.[20] The Mn-doped sodium silicide precursor was reacted with ammonium bromide to make hydrogen capped Mn-doped Si QDs following published methods.[9,13,22] The hydride-capped Si_{Mn} QDs were then refluxed with allylamine in DMF to form chemically robust Si–C bonds on the surface *via* a hydrosilylation process to protect the silicon particles from

oxidation. Propylamine capping made the QDs water soluble and easily functionalizable. Morphology and size distribution of the propylamine terminated Si_{Mn} QDs were observed by transmission electron microscope (TEM, Figure 1c). The QDs are well-dispersed in water with a size distribution of 4.3 ± 1.0 nm, similar to the Si_{Mn} QDs we reported before.[13]

2. Si_{Mn} QDs coated with dextran sulfate

The propylamine capped Si_{Mn} QDs were targeted to macrophages by coating with dextran sulfate having a molecular weight of 6,500–10,000 Da. The hydroxyl groups of dextran sulfate were activated with 4-nitrophenyl chloroformate, followed by replacement of *para*-nitro phenol anions with amine groups on the QDs to generate the designed targeted QDs (Figure 2a).[23] The crude product was purified by dialysis against deionized water for 72 hours in dialysis bag with MW cut-off of 12,000–14,000 Da. The validity of purification of DS Si_{Mn} QDs was verified by two control experiments where the starting materials dextran sulfate or uncoated Si_{Mn} QDs were dialysed against water with the same membrane. Trace or no starting material was retained in the bag, respectively, supporting the fact that only product is retained in the bag after dialysis. Successful coating was verified by infrared spectroscopy and elemental analysis of the purified product. In the infrared spectrum of DS Si_{Mn} QDs, new absorptions at 3580 cm^{-1} (N-H stretch), 1713 cm^{-1} (C=O stretch), and 1582 cm^{-1} (secondary amide N-H bending) are seen, while the absorptions of S=O groups shifted to 1258 (asymmetric stretch) and 1018 cm^{-1} (symmetric stretch) compared to the absorptions of 1265 and 1026 cm^{-1} in dextran sulfate (Supplementary Figure 1).[24] The emergence of nitrogen (1.51%) and decrease of sulfur content (from ~17% in dextran sulfate to 9.62% in product) in DS Si_{Mn} QDs further verified successful conjugation of dextran sulfate and Mn-doped Si QDs.

TEM images (Figure 2b) show the formation of nanoparticulate clusters of Mn-doped Si “core” particles within the polysaccharide coating. The average size of nanoparticle clusters was 15–30 nm and each cluster contained ~5–10 of the Mn-doped Si “cores”, as shown in the inset of Figure 2b. Dynamic light scattering (DLS) measurements of the DS Si_{Mn} QDs indicate that the hydrodynamic diameters of the clusters range from 8.3 to 43 nm (Figure 2c).

3. Optical and magnetic properties of DS Si_{Mn} QDs

The DS Si_{Mn} QDs in water fluoresce strongly when excited with single- or two-photon laser. For single-photon excitation, the emission peak is around 441 nm and the intensity of emission is maximal for excitation at 360 nm (Supplementary Figure 2). Similar to our previous results,[13,25] a slight red-shift in emission was observed with increasing excitation wavelength. The quantum yield (QY) of the QDs in water is 8.1% when compared with quinine sulfate.[26] The emission wavelength and the photoluminescence intensity of Si_{Mn} QDs did not show any significant change after dextran sulfate coating; however, luminescence efficiency was lower in water compared to the QY in organic solvent we reported before (QY: 16% in chloroform).[13] The reduction of QY during the transfer from organic phase to water may be attributed to the interaction of dipole moment of water and the electron-hole pair of the particles, giving rise to mechanisms for non-radiative decay.12 The observed QY value in water is comparable to values of QY for Si QDs reported in the literature, which range from 2–18% in water.[8–10] For two-photon excitation at the peak value of 790 nm yielded emission at ~478 nm. Signal was still detectable with 840 nm excitation (Figure 3a). To make the results insensitive to changes in laser power or pulse width, the data have been corrected according to the following equation that is derived from the nonlinear nature of the signal:

$$Signal \propto (P_m)^2 \frac{T}{\tau},$$

where P_m is the mean laser power after the microscope objective for each wavelength, τ is the previously measured pulse width,[27] and T is the pulse repetition rate (80 MHz). Obtained photoluminescence signal values were normalized by setting the highest signal value to 100.

Although Mn-containing agents have long been used as T_1-weighted contrast agents, they are non-specific and with low sensitivity. Particle-based technologies provide an efficient way to deliver high payload of metal ions and slow rotational tumbling time, generating contrast agents with high relaxivity while being thermodynamically and kinetically stable.[28] The DS Si_{Mn} QDs show promising MRI properties. They have an r_1 relaxivity of 25.50 ± 1.44 $mM^{-1}s^{-1}$ and an r_2 relaxivity of 89.01 ± 3.26 $mM^{-1}s^{-1}$ (37 °C, 1.4 T) in pH 7.0 deionized water. The relaxivities for DS Si_{Mn} QDs are much higher than the commercially available gadolinium contrast agents ($r_1 \approx 4$ $mM^{-1}s^{-1}$1) and comparable to those reported for Mn or gadolinium (Gd) nanoparticles, such as Gd^{3+} ion encapsulated in micelles or silica, attached on dendrimer, or Gd oxide nanoparticles.[29–31] The r_1 values of Mn nanoparticles, such as Mn^{2+} ion encapsulated in micelles[32,33] or Mn oxide nanoparticles,[34,35] reported in the literature are in the range of 4.1–37.5 $mM^{-1}s^{-1}$, while r_2 values are in the range of 18.9–2,585 $mM^{-1}s^{-1}$ for fields above 1.5 T. T_1- and T_2-weighted MR imaging (T_1W MRI and T_2W MRI) of a series of concentrations of the DS Si_{Mn} QDs in aqueous solution were performed at 9.4 T and showed that for T_1W MRI, the signal intensity increases significantly with the increase of manganese concentration (Figure 3b). In T_2W MRI images, the signal intensity variation is not as significant, even using longer TR and TE, indicating that the DS Si_{Mn} QDs are more suitable for T_1W MRI.[36]

4. Uptake of DS Si_{Mn} QDs by macrophages

To demonstrate targeting to macrophages by the DS Si_{Mn} QDs, we performed *in vitro* studies using P388D1 murine macrophage cells. After incubation with DS Si_{Mn} QDs, strong fluorescence is visible in the cells, as shown in Figure 4b (single photon excitation). Weak fluorescence is observed from control cells that have not been incubated with the probes (Figure 4a), verifying that the fluorescence observed in Figure 4b arises from the probes and not autofluorescence of the cells. Uptake of the DS Si_{Mn} QDs is visible as punctate spots of fluorescence in the cytoplasm of the cells (Supplementary Figure 3). This pattern of signal is consistent with an endocytic mode of internalization.[37] Cells from a parallel experiment were lysed for MRI. The contrast between cell lysate containing probes and blank cell lysate is significant in T_1W MR images when a 0.02 mM of Mn concentration of QD was applied to cells as shown in Figures 4a and 4b. On the other hand, no significant difference is observed by T_2W MRI. Control QDs were prepared from the same batch of Si_{Mn} QDs but coated with non-sulfated dextran (D Si_{Mn} QDs), which is not recognized by the receptor. Both optical imaging and T_1W MRI images (Figure 4c) show that there was very limited uptake of D Si_{Mn} QDs compared to the targeted probes.

The results showed that DS Si_{Mn} QDs generated significant image contrast for macrophages at low Mn concentration (0.02 mM). This concentration is comparable to that found in a recent study performed by Viglianti *et al.* who used MRI to monitor tissue pharmacokinetics of a liposome/drug *in vivo*. They found that, *in vivo*, MR sensitivity requires a Mn^{2+} ion concentration of at least 0.0175 mM (post-release) in tissue to obtain adequate contrast. Thus, our result indicates that cells can readily accumulate DS Si_{Mn} QD's at sufficient density to allow for T_1W MRI *in vivo* measurements.

Direct two-photon imaging at 780 nm excitation was performed, as shown in Figure 5. The macrophage cells were fixed and imaged with a Zeiss LSM 510NLO microscope. Similar to the result of single photon microscopy, strong fluorescence is visible in the cells (Figure 5a) after incubation with DS Si_{Mn} QDs. Uptake of the DS Si_{Mn} QDs is visible as punctate spots of fluorescence in the cytoplasm of the cells (Figure 5b), which is consistent with an endocytic

mode of internalization. No fluorescence is observed from control cells that have not been incubated with the probes, verifying that the fluorescence observed in Figure 5 arises from the probes and not autofluorescence of the cells. This figure demonstrates that two photon imaging of Si QD is possible *in vitro* and that DS Si_{Mn} QDs accumulate in vesicles of the cells.

QDs are usually excited at short wavelengths which can induce photodamage, autofluorescence, and light scattering, therefore hampering their applications in dense tissue imaging. Multiphoton excitation at red and NIR light, where tissues are relatively transparent, is especially useful for optical imaging. Recent advances in 2-photon techniques have greatly improved the penetration ability of optical microscopy, for example, up to 900 μm in recording blood flow speed in individual cortical vessels,[38] 500–750 μm into the brain,[39] and 500 μm down in dense lymph nodes.[40] Multiphoton microscopy of QDs have been successfully used for imaging a variety of diseases, such as long-term *in vivo* imaging of synaptic plasticity in adult cortex,[41] or the analysis of physiological function and angiogenesis *in vivo* tumor biology, [42,43] etc. Recently, He and co-workers reported multiphoton excitation of Si QDs in water.[44] However, cell imaging and relevance to biological materials using Si QDs has not been reported. Our results show that macrophages with DS Si_{Mn} QDs fluoresce strongly when excited at 780 nm, enabling long-term imaging of cellular processes with reduced photodamage compared to UV-excited imaging. This will greatly enhance the potential of Si QDs for use as biological probes for *in vivo* imaging.

5. Competitive uptake of DS Si_{Mn} QDs by macrophages

As described earlier the probes are targeted to cells through the macrophage scavenger receptor class A (SR-A). The scavenger receptor is a high affinity receptor present in high numbers on macrophages. They are not down-regulated with ligand concentration, mediate very efficient and rapid internalization of bound ligand, and repeatedly recycle *via* endocytic compartments, illustrating desirable traits as targets for labeling.[16] Specificity of cellular uptake was confirmed by competition studies in which cells were incubated with a fixed concentration of DS Si_{Mn} QDs and increasing excess of unlabeled dextran sulfate. If uptake were receptor-mediated, the excess unlabeled ligand should compete for uptake. Nonspecific uptake is strictly concentration-dependent and would not be affected by additional ligands in the solution.[16] Receptor-mediated uptake is confirmed by the results seen in Figure 6: increasing amounts from 0.1 to 10-fold excess competitor strongly reduce uptake as expected for a receptor-mediated process.

Competitive inhibition studies strongly support that the enhancement observed by DS Si_{Mn} QDs is directly related to specific uptake *via* the macrophage scavenger receptor. Specific uptake is further confirmed by control experiments showing limited contrast enhancement when using non-targeted D Si_{Mn} QDs, similar to the enhancement observed when using dextran coated iron oxide particles for imaging atherosclerotic plaques, which accumulate in macrophages by nonspecific phagocytosis and passive diffusion.[45] We have previously developed dextran sulfate coated iron oxide nanoparticles based on a noncovalent co-precipitation procedure.[46,47] This is the first example of covalently bonding dextran sulfate to the surface of a QD; this targeted QD demonstrated much better contrast than nontargeted D Si_{Mn} QDs synthesized as controls.

Macrophages and macrophage scavenger receptor (MSR) play a key role in the pathogenesis of atherosclerosis. Macrophages are present through all stages of atherosclerosis development, from the initiation of plaques through the formation of complex plaques containing foam cells, lipid accumulations, necrotic debris, and thrombus, and have been specifically associated with plaque stability—high densities of macrophages correlate with vulnerability to rupture. The specific uptake of DS Si_{Mn} QDs by macrophages *via* scavenger receptor suggests favorable potential for using DS Si_{Mn} QDs in the detection of vulnerable plaques found in atherosclerosis.

6. Cytotoxicity of DS Si_{Mn} QDs to mammalian cells

As a preliminary assessment of the toxicity, DS Si_{Mn} QDs were applied to P388D1 cells in culture and the cell viability was evaluated by the C_{12} - Resazurin viability assay.[21] The average cell viability is 90% after 24 h incubation with the QDs varying from 0.01 to 0.11 mM of manganese concentration. For confirmation, the same experiments were performed on another mammal cell line, NIH 3T3 cells. The average NIH 3T3 cell viability is 97% after 24 h incubation with the concentration of QDs varying from 0.01 to 0.12 mM of manganese, indicating that the DS Si_{Mn} QDs are non-toxic to mammal cells at concentrations needed for image contrast (Figure 7).

A major concern that limits the use of QDs in clinic is the toxicity associated with the cadmium in QDs. The Si-based nanoparticles hold exciting potential for clinical applications due to their lack of toxicity compared to cadmium based QDs. Si has an LD_{50} of 3160 mg/kg compared with 88 mg/kg for Cd^{2+} (chloride) and 450 mg/kg for iron (ferric chloride) for oral ingestion in the rat model. Studies on porous Si films have shown that the primary decomposition product is orthosilicic acid ($Si(OH)_4$), which is a component for normal bone and connective tissue homeostasis. The additional $Si(OH)_4$ does not adversely affect homeostasis.[48,49] Our study showed that DS Si_{Mn} QDs at concentrations relevant for biological imaging do not have observable toxicity to mammalian cells, further confirming the biocompatibility of Si-based nanoparticles.

Conclusion

Water soluble Mn doped Si QDs have been synthesized and successfully conjugated with dextran sulfate. In these studies we demonstrate that the dextran sulfate coated Si_{Mn} QDs significantly enhance signal from macrophages in both MR and fluorescence images. DS Si_{Mn} QDs are not toxic to mammalian cells. In addition, we demonstrate that DS Si_{Mn} QDs can be imaged in cells using two-photon NIR imaging. To our knowledge, the work presented here is the first example demonstrating that Si QDs in cells are detectable by two-photon imaging. Nanotechnology offers an exciting possibility of integrating multiple properties in a single imaging contrast agent. Multifunctional nanobiomaterials detected by highly complementary anatomical and molecular based imaging capabilities can allow simultaneous data acquisition, accurate image co-registration, and more meaningful interpretation of data.[50] Such multimodal methods hold great promise for improving diagnosis/therapy of diseased states, and represent the next stage of contrast agent development for non-invasive molecular imaging. The method presented is a general synthetic method that can be easily modified with specific ligands to label other biomarkers in atherosclerotic plaques, such as VCAM-1 and thrombus, etc, or to detect other diseases such as cancer. Further studies are underway to more fully characterize the behavior and localization of the probe in biological systems and move the probe towards *in vivo* applications.

Supplementary Material

Refer to Web version on PubMed Central for supplementary material.

Acknowledgments

The authors wish to acknowledge the National Institute of Health (HL081108-01, EB008576-01, and EB006192), a German Science Foundation (DFG) Postdoctoral Fellowship, and the NMR award of the University of California, Davis for support of this work. We thank Dr. Xiaobo Liu for help in two-photon imaging.

References

(1). Weissleder R, Pittet MJ. Nature 2008;452:580–589. [PubMed: 18385732]

(2). Cheon J, Lee JH. Accounts Chem. Res 2008;41:1630–1640.
(3). Kim J, Piao Y, Hyeon T. Chem. Soc. Rev 2009;38:372–390. [PubMed: 19169455]
(4). Mulder WJM, Griffioen AW, Strijkers GJ, Cormode DP, Nicolay K, Fayad ZA. Nanomedicine 2007;2:307–324. [PubMed: 17716176]
(5). Resch-Genger U, Grabolle M, Cavaliere-Jaricot S, Nitschke R, Nann T. Nat. Methods 2008;5:763–775. [PubMed: 18756197]
(6). Derfus AM, Chan WCW, Bhatia SN. Nano Lett 2004;4:11–18.
(7). O'Farrell N, Houlton A, Horrocks BR. Int. J. Nanomed 2006;1:451–472.
(8). Warner JH, Hoshino A, Yamamoto K, Tilley RD. Angew. Chem.-Int. Edit 2005;44:4550–4554.
(9). Zhang XM, Neiner D, Wang SZ, Louie AY, Kauzlarich SM. Nanotechnology 2007;18
(10). Erogbogbo F, Yong KT, Roy I, Xu GX, Prasad PN, Swihart MT. ACS NANO 2008;2:873–878. [PubMed: 19206483]
(11). Sudeep PK, Page Z, Emrick T. Chem. Commun 2008:6126–6127.
(12). Wang S, Jarrett BR, Kauzlarich SM, Louie AY. J. Am. Chem. Soc 2007;129:3848–3856. [PubMed: 17358058]
(13). Zhang X, Brynda M, Britt RD, Carroll EC, Larsen DS, Louie AY, Kauzarich SM. J. Am. Chem. Soc 2007;129:10668–+. [PubMed: 17691792]
(14). Sanz J, Fayad ZA. Nature 2008;451:953–957. [PubMed: 18288186]
(15). Choudhury RP, Fisher EA. Arterioscler. Thromb. Vasc. Biol 2009;29:983–991. [PubMed: 19213945]
(16). Gustafsson B, Youens S, Louie AY. Bioconjugate Chem 2006;17:538–547.
(17). de Winther MPJ, van Dijk KW, Havekes LM, Hofker MH. Arterioscler. Thromb. Vasc. Biol 2000;20:290–297. [PubMed: 10669623]
(18). Ma XC, Wu FY, Kauzarich SM. J. Solid State Chem 2008;181:1628–1633.
(19). Ma XC, Xu F, Atkins TM, Goforth AM, Neiner D, Navrotsky A, Kauzlarich SM. Dalton Trans 2009:10250–10255. [PubMed: 19921060]
(20). Goebel T, Prots Y, Haarmann F. Zeitschrift Fur Kristallographie-New Crystal Structures 2008;223:187–188.
(21). O'Brien J, Wilson I, Orton T, Pognan F. Eur. J. Biochem 2000;267:5421–5426. [PubMed: 10951200]
(22). Neiner D, Chiu HW, Kauzlarich SM. J. Am. Chem. Soc 2006;128:11016–11017. [PubMed: 16925406]
(23). Heinze, T.; Liebert, T.; Heublein, B.; Hornig, S. Polysaccharides Ii. Vol. Vol. 205. Springer-Verlag Berlin; Berlin: 2006. p. 199-291.
(24). Ramirez JC, Sanchezchaves M, Arranz F. Angew. Makromol. Chem 1995;225:123–130.
(25). Zhang XM, Neiner D, Wang SZ, Louie AY, Kauzlarich SM. Nanotechnology 2007;18:6.
(26). Lakowicz, JR. Principles of Fluorescence Spectroscopy. 2nd ed.. Kluwer Academic/Plenum Publishers; New York, London, Moscow, Dordrecht: 1999.
(27). Dickinson ME, Simbuerger E, Zimmermann B, Waters CW, Fraser SE. J. Biomed. Opt 2003;8:329–338. [PubMed: 12880336]
(28). Castelli DD, Gianolio E, Crich SG, Terreno E, Aime S. Coord. Chem. Rev 2008;252:2424–2443.
(29). Sharma P, Brown SC, Walter G, Santra S, Scott E, Ichikawa H, Fukumori Y, Moudgil BM. Adv. Powder Technol 2007:663–698.
(30). Hermann P, Kotek J, Kubicek V, Lukes I. Dalton Trans 2008:3027–3047. [PubMed: 18521444]
(31). Caravan P, Ellison JJ, McMurry TJ, Lauffer RB. Chem. Rev 1999;99:2293–2352. [PubMed: 11749483]
(32). Unger E, Fritz T, Shen DK, Wu GL. Invest. Radiol 1993;28:933–938. [PubMed: 8262748]
(33). Taylor KML, Rieter WJ, Lin WB. J. Am. Chem. Soc 2008;130:14358–+. [PubMed: 18844356]
(34). Mertzman JE, Kar S, Lofland S, Fleming T, Van Keuren E, Tong YY, Stoll SL. Chem. Commun 2009:788–790.
(35). Pan DPJ, Senpan A, Caruthers SD, Williams TA, Scott MJ, Gaffney PJ, Wickline SA, Lanza GM. Chem. Commun 2009:3234–3236.

(36). Bock NA, Paiva FF, Silva AC. NMR Biomed 2008;21:473–478. [PubMed: 17944008]

(37). Koval M, Preiter K, Adles C, Stahl PD, Steinberg TH. Exp. Cell Res 1998;242:265–273. [PubMed: 9665824]

(38). Kobat D, Durst ME, Nishimura N, Wong AW, Schaffer CB, Xu C. Opt. Express 2009;17:13354–13364. [PubMed: 19654740]

(39). Wilt BA, Burns LD, Ho ETW, Ghosh KK, Mukamel EA, Schnitzer MJ. Annu. Rev. Neurosci 2009;32:435–506. [PubMed: 19555292]

(40). Makale M, McElroy M, O'Brien P, Hoffman RM, Guo S, Bouvet M, Barnes L, Ingulli E, Cheresh D. Journal of Biomedical Optics 2009;14:024032. [PubMed: 19405761]

(41). Trachtenberg JT, Chen BE, Knott GW, Feng G, Sanes JR, Welker E, Svoboda K. Nature 2002;420:788–94. [PubMed: 12490942]

(42). Brown EB, Campbell RB, Tsuzuki Y, Xu L, Carmeliet P, Fukumura D, Jain RK. Nat Med 2001;7:864–8. [PubMed: 11433354]

(43). Larson DR, Zipfel WR, Williams RM, Clark SW, Bruchez MP, Wise FW, Webb WW. Science 2003;300:1434–1436. [PubMed: 12775841]

(44). He GS, Zheng QD, Yong KT, Erogbogbo F, Swihart MT, Prasad PN. Nano Lett 2008;8:2688–2692. [PubMed: 18698830]

(45). Amirbekian V, Lipinski MJ, Briley-Saebo KC, Amirbekian S, Aguinaldo JGS, Weinreb DB, Vucic E, Frias JC, Hyafil F, Mani V, Fisher EA, Fayad ZA. Proc. Natl. Acad. Sci. U. S. A 2007;104:961–966. [PubMed: 17215360]

(46). Jarrett BR, Frendo M, Vogan J, Louie AY. Nanotechnology 2007;18

(47). Jarrett BR, Gustafsson B, Kukis DL, Louie AY. Bioconjugate Chem 2008;19:1496–1504.

(48). Anderson SHC, Elliot H, Wallis DJ, Canham LT, Powell JJ. Phys. stat. sol. (a) 2003;197:331–335.

(49). Fujioka K, Hiruoka M, Sato K, Manabe N, Miyasaka R, Hanada S, Hoshino A, Tilley RD, Manome Y, Hirakuri K, Yamamoto K. Nanotechnology 2008;19:7.

(50). Niedre M, Ntziachristos V. Proc. IEEE 2008;96:382–396.

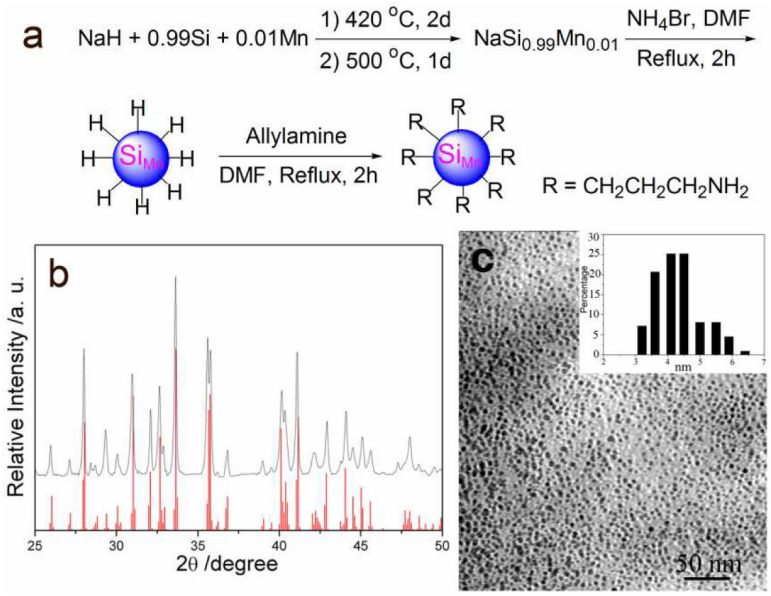

Figure 1.

(a) Synthesis of propylamine coated Mn-doped Si QDs (Si_{Mn} QDs); (b) XRD pattern of the product from optimized reactions of NaH, Si, and Mn. The red lines indicate the X-ray diffraction peak position for calculated Na_4Si_4; (c) TEM images of amine-terminated Si_{Mn} QDs, and the inset is the size distribution of QDs.

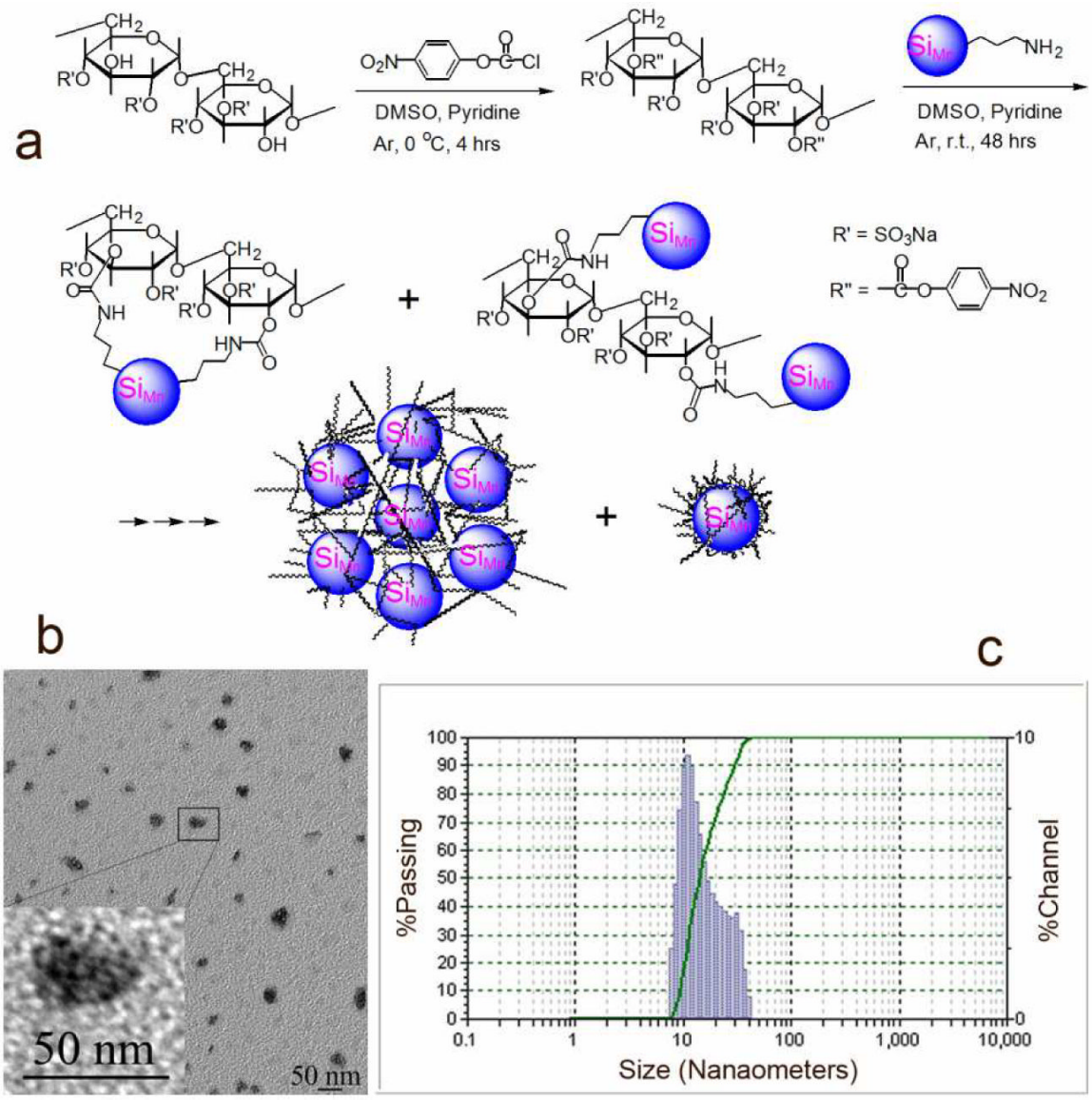

Figure 2.

(a) Synthesis of dextran sulfate coated Mn-doped Si QDs (DS Si_{Mn} QDs); (b) TEM images of DS Si_{Mn} QDs, and the inset is the enlarged TEM image of DS Si_{Mn} QDs (darker cores distributed in a lighter matrix); and (c) hydrodynamic size of DS Si_{Mn} QDs measured by DLS.

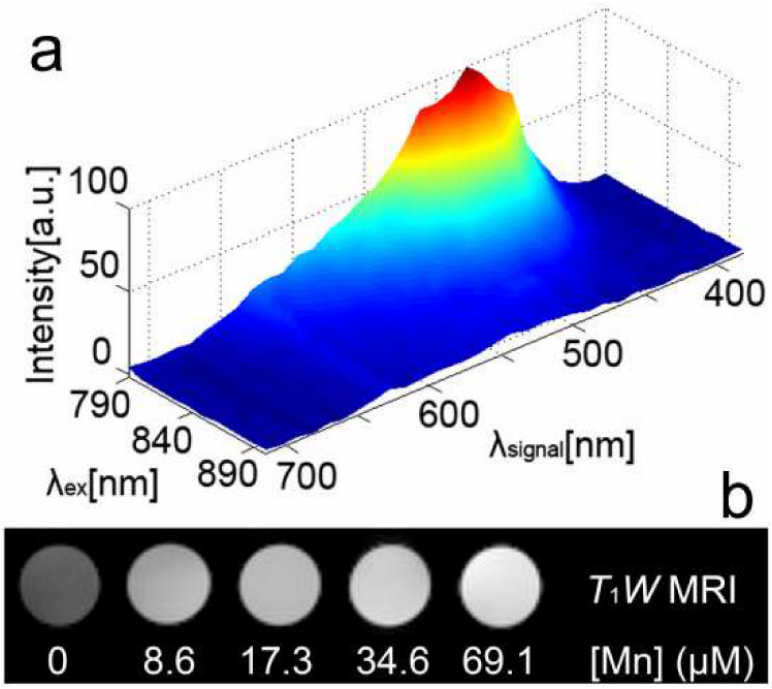

Figure 3.

(a) Two-photon 3D normalized luminescence signal data profile of DS Si_{Mn} QDs at different excitation wavelengths in water. The background signal measured in a random region without DS Si_{Mn} QDs was subtracted. Color code: dark blue corresponds to zero intensity and dark red corresponds to maximal intensity; (b) The DS Si_{Mn} QDs aqueous solutions imaged by MRI show different brightness depending on the manganese concentration.

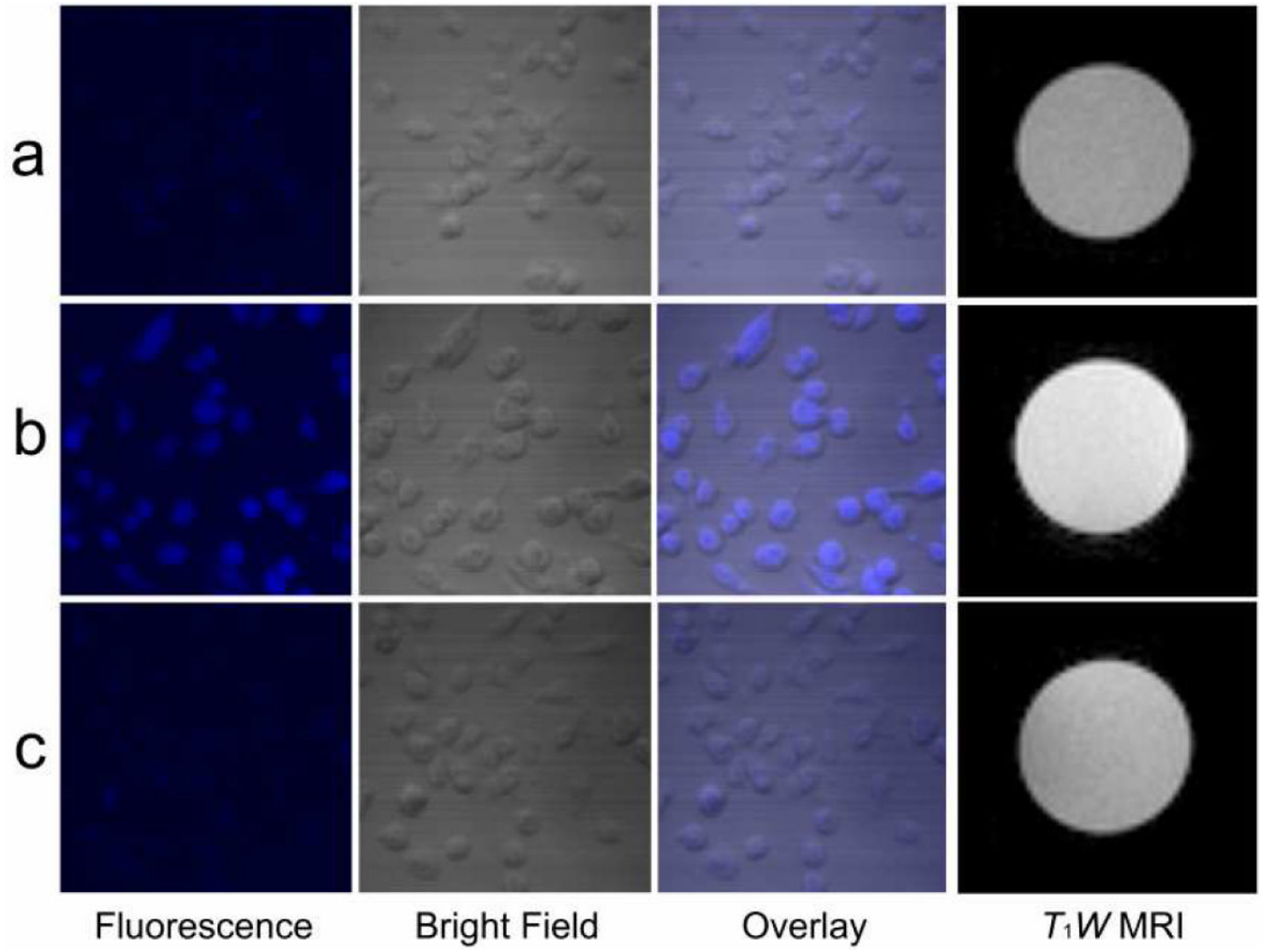

Figure 4.
Confocal imaging and T_1W MRI of (a) blank P388D1 cells, (b) DS Si_{Mn} QDs in P388D1 cells, and (c) D Si_{Mn} QDs in P388D1 macrophage cells. ($[Mn^{2+}] = 2 \times 10^{-5}$ M).

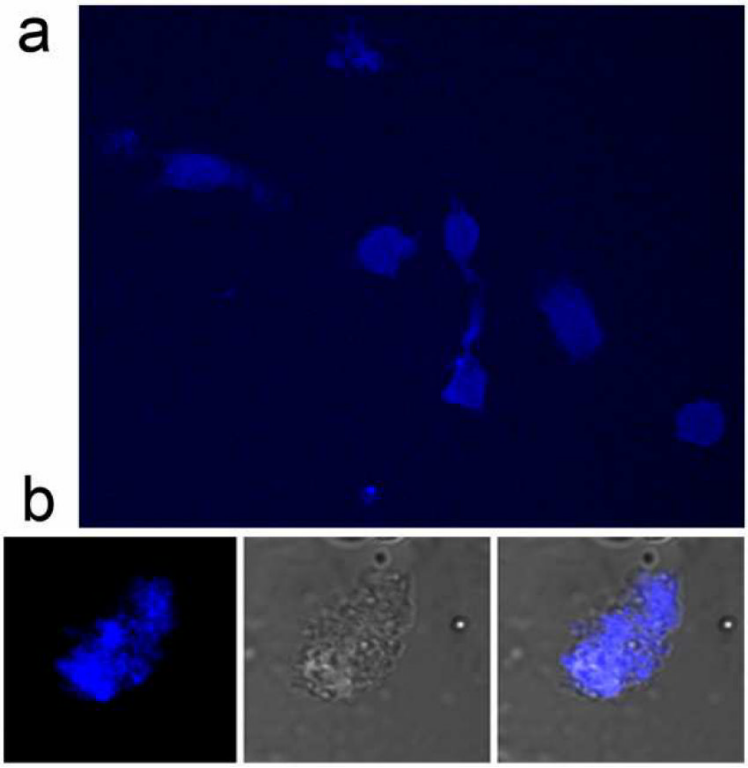

Figure 5.
Two-photon images of P388D1 macrophage cells treated with DS Si_{Mn} QDs ($[Mn^{2+}] = 2 \times 10^{-5}$ M) with excitation at 780 nm.

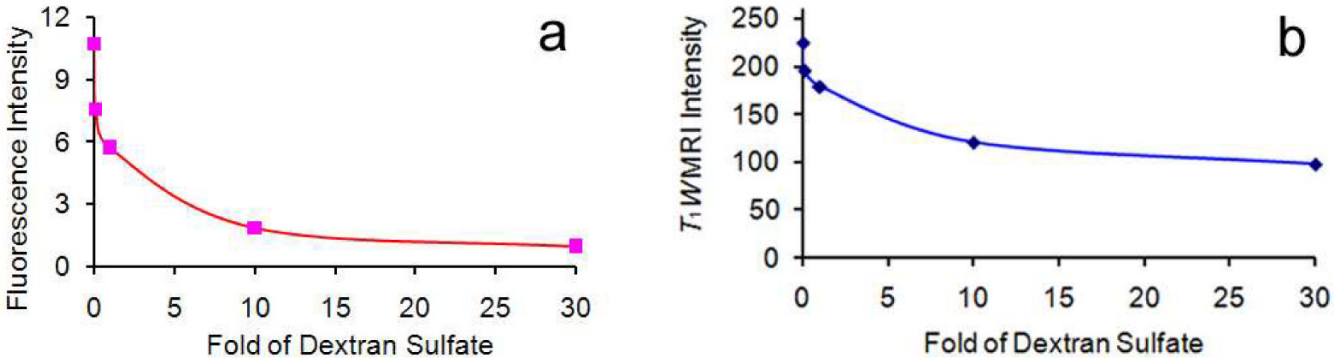

Figure 6.

Competitive uptake of DS Si_{Mn} QDs ($[Mn^{2+}] = 1.64 \times 10^{-5}$ M) and dextran sulfate by P388D1 cells. The fluorescence (a) and MRI (b) plots are given as mean signal intensity (arbitrary units) for each sample measured by *Image J*.

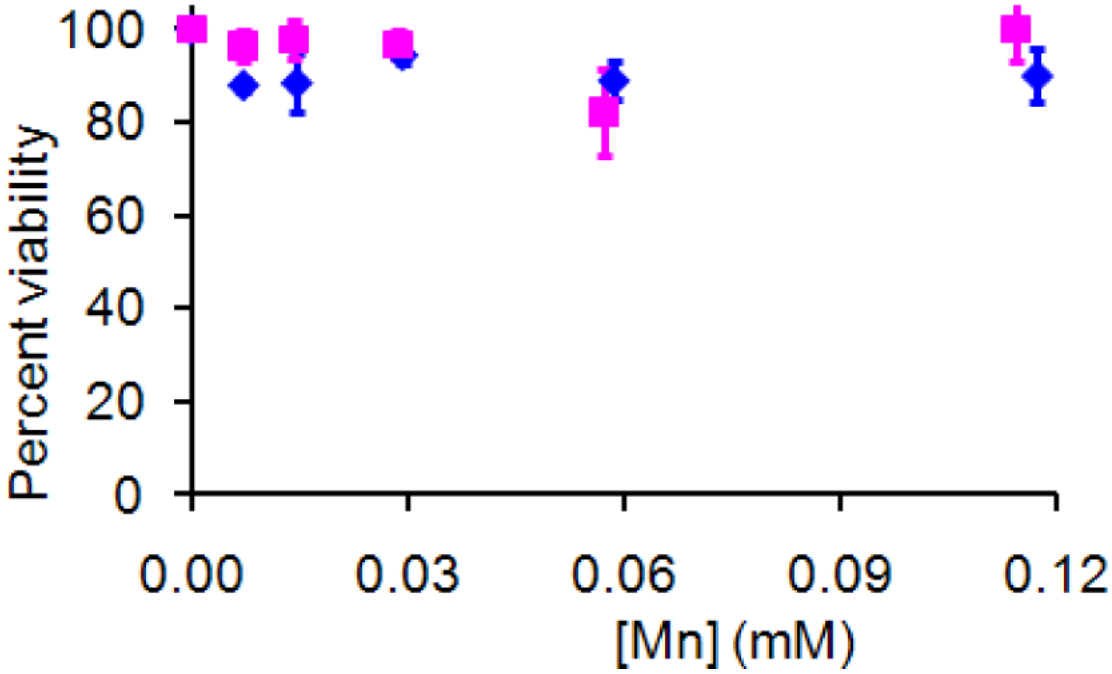

Figure 7.
Cytotoxicity after 24 h incubation with DS Si_{Mn} QDs in P388D1 cells (■), and NIH 3T3 cells (◆).